ORNL-2544
Metallurgy and Ceramics

CORRELATION OF CAVITATION INCEPTION DATA FOR A CENTRIFUGAL PUMP OPERATING IN WATER AND IN SODIUM POTASSIUM ALLOY (NaK)

A. G. Grindell

OAK RIDGE NATIONAL LABORATORY · U.S. ATOMIC ENERGY COMMISSION

OAK RIDGE NATIONAL LABORATORY
operated by
UNION CARBIDE CORPORATION
for the
U.S. ATOMIC ENERGY COMMISSION

Printed in USA. Price 150 cents. Available from the

Office of Technical Services
U. S. Department of Commerce
Washington 25, D. C.

ORNL-2544

Contract No. W-7405-eng-26

REACTOR PROJECTS DIVISION

CORRELATION OF CAVITATION INCEPTION DATA FOR A CENTRIFUGAL PUMP OPERATING IN WATER AND IN SODIUM POTASSIUM ALLOY (NaK)

A. G. Grindell

DATE ISSUED

DEC 11 [illegible]

OAK RIDGE NATIONAL LABORATORY
Oak Ridge, Tennessee
operated by
UNION CARBIDE CORPORATION
for the
U.S. ATOMIC ENERGY COMMISSION

CONTENTS

CORRELATION OF CAVITATION INCEPTION DATA FOR A CENTRIFUGAL PUMP OPERATING IN WATER AND IN SODIUM-POTASSIUM ALLOY (NaK)

A. G. Grindell

ABSTRACT

For the centrifugal pump under investigation, the static head at pump suction, in feet absolute, at cavitation inception was correlated for water and for 1500°F NaK on the basis of the differences of the vapor pressures of the two liquids. The difference between the vapor pressure of water and NaK, for the same conditions of pump speed and liquid flow, was added to the water-test cavitation inception value, and this estimate proved to be a good approximation to the experimental value found for cavitation inception with NaK.

INTRODUCTION

In view of the expanding use of nonaqueous heat-transfer media in power generation, it would be desirable, from the viewpoint of economy and convenience, to be able to predict the inception of pump cavitation for nonaqueous systems by using the wealth of information which has been obtained for aqueous systems. (Cavitation in a flowing liquid is described as the vaporization of the liquid when the static pressure is reduced to or below the vapor pressure of the liquid at the local temperature of the flowing liquid.) The operation of a centrifugal pump in a region of cavitation can lead to a reduction in pump performance and damage to the impeller and casing.

Some work has been reported on cavitation in liquid metals, but none has been related to cavitation in water. Hall and Crofts (*1*) and Trummel (*2*) have reported on cavitation in liquid metals. Both reports concerned cavitation in a venturi; Hall and Crofts worked with eutectic sodium-potassium alloy at 250°C, and Trummel worked with sodium at 1215- to 1475°F. A. J. Stepanoff (*3*) has reported on the density dependence of cavitation suppression for propeller pumps in a molten salt of sp gr 1.75 at 850°C. On page 257 of his textbook (*4*), Stepanoff writes, "Vapor pressure should not be overlooked with liquids other than water." Allis-Chalmers Manufacturing Company (*5*) has reported on a study of cavitation damage to specimens of various materials of construction in 70°F water, 350°F sodium, and 350°F eutectic sodium-potassium alloy. Studies similar to the Allis-Chalmers work have been made in the Experimental Engineering Department of the Reactor Projects Division, ORNL, by Young and Simpson (*6*). That work is not presented here because the semi-quantitative nature of the measurements of pump speeds, flows, and temperatures precluded applicability to the establishment of the correlation between nonaqueous and aqueous systems.

In high-temperature heat-exchanger circuits, the working pressure of system components, and consequently their design, will depend upon, among other considerations, the pressure necessary to suppress pump cavitation. It would be valuable to be able to predict centrifugal-pump cavitation inception in sodium-potassium alloys early in the design study by adapting water cavitation data which appears in large quantities in the literature. Experiments with heat transfer media other than sodium-potassium alloys may expand the application of water-cavitation data to nonaqueous systems.

In order to discover whether a useful relationship exists between centrifugal-pump cavitation inception in water and in a molten metal, a centrifugal pump was used, first in water, and then in 1500°F NaK (56 wt % Na–44 wt % K). Five test points of pump operation were chosen; three runs were made at 300 gal/min for pump speeds of 2600, 3000, and 3375 rpm, and two runs were made at 430 gal/min for pump speeds of 3000 and 3375 rpm. One run was made at each of the five test points for water and for NaK. Two additional runs were made with NaK for each of the two flow conditions at 3000 rpm. Cavitation damage was not investigated.

A sufficient number of reductions in pump-tank gas pressure (helium, under pressure, was used as a protective cover for the NaK) were made in order to identify the cavitation inception point, H_{ci}, on a plot of H_t vs H_{ss} (see Glossary) and to obtain a loss of at least 8 ft of pump head.

PROCEDURE

EQUIPMENT

The development of pumps for specific applications has been part of the component development work of the Experimental Engineering Department of the Reactor Projects Division of ORNL. A centrifugal pump developed by the Department for pumping high-temperature NaK was installed in a closed loop of Inconel pipe, sched 40, 4-in. IPS. The loop was equipped with thermocouple, venturi flow meter, throttling valve, pressure measuring devices, heaters and coolers providing for isothermal operation, oxide-removal cold trap, thermal insulation, drain valve, drain tank, pump-speed measuring devices and devices for measuring the level of the liquid in the pump tank. Figure 1 is a sketch of the test setup.

TEST METHOD

In general, the method for obtaining cavitation data and the types of data obtained were identical for both water and high-temperature NaK. The pump was operated in a noncavitating manner for the speed, flow, and temperature requirements of a selected test point. Data were obtained on pump speed, liquid flow-rate, pump head, static head at pump suction, and temperature of the liquid after each of several successive reductions in pump-tank gas pressure (static head at pump suction). A sufficient number of reductions in pump-tank gas pressure (helium, under pressure, was used as a protective cover for the NaK) were made in order to identify the cavitation inception point, H_{ci}, on a plot of H_t vs H_{ss} (see Glossary). The data were corrected by using the appropriate calibration corrections, and graphs (see Fig. 3 for typical graph) were plotted of pump head (measured in feet) vs static head at pump suction (measured in feet absolute) for each run. The static head at pump suction at the inception of cavitation was determined for each run from the corresponding graph. The difference between the vapor pressure of water and NaK was added to the water-test cavitation inception value, and this value was compared with the corresponding NaK-test cavitation inception value.

The flow rates of both water and NaK were measured by using the same venturi flowmeter. The flow rate of the NaK was based on the product of the water venturi-meter differential pressure multiplied by the square of the temperature multiplier (*TM*). Appendix *A* presents a derivation of the temperature multiplier from the standard flowmeter equation for a venturi. The underlying assumption for this particular application of the temperature multiplier method is that the venturi coefficient-of-discharge (c) varies insignificantly in value between the water and the alloy tests. The discharge coefficient varies from approximately 0.9915 for water flow-rate measurements to approximately 0.9940 for NaK flow-rate measurements (7). Table 6 presents the venturi temperature-multiplier, which includes changes in density, for three temperatures of interest. The purpose of setting the flow rates of the alloy in this manner was to duplicate as closely as practicable the flow rates of the water and to permit the absolute flow rates to approach the nominal values of 300 and 430 gpm.

DISCUSSION OF TEST VARIABLES

The principal variables of interest were pump-shaft speed, liquid flow-rate, pump-tank gas pressure, pump discharge-pressure, and liquid temperature. The method of measuring each of these quantities for water and for high-temperature NaK will be discussed in this section.

The pump-shaft speed for the water test was measured by two methods. A Strobotac adjusted to line frequency at 3600 rpm was used to stop an image of the pump-shaft coupling at the desired speed. In addition, a count-rate meter was used to integrate, for a selected period of time, the voltage pulses of the pump drive-motor tachometer generator. The integrated number of pulses was then reduced to pump-shaft speed by use of a multiplier which reflected the number of pulses per revolution of the shaft and the selected time period.

Pump-shaft speed for the high-temperature run was measured by various methods. For the 3000 rpm run, a Strobotac operating on line frequency was used to obtain a particular image from a pattern of marks which had been painted on the periphery of the pump-shaft coupling. This speed was checked by two methods, one being the count-rate meter mentioned above. A second check was performed by using a Hewlett-Packard counter, Model 522B. The three methods agreed to within 5 rpm. Other pump-shaft speeds which were not multiples of 300 were measured in the following manner. The pump-shaft speed was set at the speed multiple of 300 rpm nearest the desired test speed by using the Strobotac operating on line frequency in order to obtain the image particular to that multiple. This particular speed was then used to check the readings of both the Hewlett-Packard instrument and the count-rate meter. The shaft speed was then adjusted to the desired speed for the test and was checked by each of the three methods. A measurement range of 10 rpm at the test speed was observed.

The flow rate of the water was measured with a nozzle-type venturi meter having a single pressure tap in the pipe and one in the throat. These two pressures were measured individually with laboratory-type test pressure gages. The gages were checked at least twice during the water tests and had a maximum error of 0.3 psig at the maximum gage reading.

The flow rate of the alloy was measured with the same venturi meter used for the water tests. The venturi pipe and throat pressures were measured with bellows-actuated balanced-pressure transmitters connected to receiving gages. These pressure-measuring devices were calibrated four times during the course of high-temperature testing. The calibrations were made at zero pump speed by increasing the gas pressure in the pump (expansion) tank in increments of approximately 10 psi and by recording for each step the reading of the individual receiving gage. During these calibrations, the pump-tank gas pressure was measured with a master gage which had been calibrated by the dead-weight test method. The receiving-gage readings for each pressure-measuring device were corrected to the master-gage reading, and the corrections were plotted. A smooth curve was drawn through the correction points. An analysis, based on each of three pressure-measuring-device calibrations, was made of the alloy flow rates. The maximum deviations of the probable actual alloy flow rate from the desired flow rate, taken from the corresponding water run, were calculated to be +5 gpm and −5 gpm for alloy runs 3A and 5, respectively.

The gas pressure of the pump tank was measured with a 0–30 psig laboratory-type test gage. The gage was calibrated against the dead-weight-tested master gage, and the maximum error in the range of interest was 0.10 psig. The pump-tank gas pressure data were not corrected.

The discharge pressure of the pump was measured with a bellows-actuated balanced-pressure transmitter connected to a receiving gage. An analysis, based on each of three pump-discharge measuring-device calibrations, was made of the pump head. The largest deviation in pump head, based on the three calibrations, was +1.1 ft. The discharge-pressure data were corrected by using one of the calibrations.

During the water cavitation tests, the system temperature was measured with a dial type of Taylor thermometer inserted into the flowing liquid. The thermometer was calibrated (*8*) after the conclusion of the water tests and was found to be reading 2°F high. The water-temperature data were corrected to this calibration.

The temperature of the NaK entering the pump suction was measured during high-temperature testing by means of a Chromel-Alumel thermocouple attached to the outside of the suction pipe. Subsequently, the thermocouple was calibrated in place against a Pt, Pt-10% Rh thermocouple which had been calibrated against an NBS thermocouple (*9*). The calibration indicated that the Chromel-Alumel temperature data were 7°F high, and this correction was used in obtaining the vapor pressure of the NaK. The suction pipe was thermally insulated with 3 in. of Superex (Johns-Manville Co.) pipe insulation. The temperature gradient through the wall of the pipe was estimated to be about 0.9°F and was not used to correct the temperature reading of the alloy which entered the pump inlet.

DISCUSSION OF THE EXPERIMENT

The water tests proceeded smoothly except that attempts to induce cavitation at the lowest speed, 2600 rpm and higher flow, 430 gpm, caused oscillations in the system-pressure levels, and the water became gassy. The gassing may have been the result of a disturbance to the normal liquid leakage (Fig. 2) which flows from the discharge region of the impeller inward across the top side of the impeller and into the free liquid surface in the pump tank. The direction of the leakage may be reversed when the head developed by the top side of the impeller exceeds the static pressure at the periphery of the impeller. The reversal in leakage flow may lead to the pumping of gas into the system by the top side of the impeller. The remedy may possibly be found in a change in the head-producing ability of the top side of the impeller in order to forestall the reversal of leakage flow at pump application conditions. Water cavitation run No. 4 may have experienced some gassing coincidental to cavitation. There was no evidence of gassing in the other water tests.

In view of the interest in NaK systems using insert-gas blankets, a discussion of the problem of self-gassing in the pumps is in order.

In the initial high-temperature test, nearly every attempt to induce cavitation led to oscillations in the system-pressure levels and to flooding of the upper reaches of the pump tank with the hot NaK. The difficulty was thought to arise from the introduction of helium into the impeller inlet, and the source of the helium was thought to be the cold trap used for oxide removal. In this device, a small portion, about 1.5 gpm, of the circulating 1500°F NaK is cooled to a relatively low temperature, 250–350°F, in order to remove sodium oxide and is then returned to the system in the pump suction line (Fig. 1). It was postulated, with the assistance of G. M. Watson, Materials Chemistry Division, ORNL, that the temperature dependence of helium solubility in NaK accounted for the helium in the pump tank. That is, helium may be more soluble in 1500°F NaK in the pump tank than in the 250–350°F NaK in the cold trap. The temperature dependence of the solubility of helium in NaK may be similar to that of helium in liquid bismuth. As measured by Watson, the solubility of helium in liquid bismuth at a given pressure increases with an increase in temperature. Accordingly, valving the cold trap out of the system was sufficient to prevent gassing the pump from that source during subsequent high-temperature operation.

Attempts to induce pump cavitation during a high-temperature run at 2600 rpm and 430 gpm produced oscillations in the system-pressure level and a rapid rise in the liquid level in the pump tank in a manner very similar to the water-gassing incident described above.

The oxide level in the circulating NaK increased from approximately 30 ppm, the value at the time the cold trap was isolated from the system, to approximately 225 ppm at the conclusion of the test.

VAPOR PRESSURE AND SPECIFIC GRAVITY OF WATER AND OF NaK

The vapor pressure and the sp gr of water for the temperature range of interest are presented in Fig. 17. The values were taken from the standard reference (*10*).

The vapor pressure of NaK, as predicted by Raoult's law, and the specific gravity of the alloy, are presented in Fig. 18. Experimental work by Miller, Ewing, *et al.* (*11*) indicated that the vapor pressure of the alloy may be slightly higher at a given temperature than would be predicted by Raoult's law. Figure 19 presents, for a temperature range of interest, the vapor pressure of the alloy as predicted by Raoult's law and as experimentally checked by Miller and Ewing (*11*). For the purposes of this correlation experiment, the average of the two values was used. The values for the sp gr of the alloy were taken from p 34 of ref (*12*).

RESULTS AND DISCUSSION

TEST DATA REDUCTION

The water-test data and computations for each run are presented in Tables 2 and 3, respectively. The data for the NaK runs and the computations for each run are shown in Tables 4 and 5, respectively. Data for the test points (P_{pt}) are shown in the horizontal rows in Tables 2 and 4. The first horizontal row of a run presents the data for the first point of the run. The computations for each test point (P_{pt}) are shown in the vertical columns in Tables 3 and 5. The first vertical column of a run represents the computations for the first point of the run.

For all tests, the average pump speed for each run was set forth as the speed of that run, and the average flow from the noncavitation region to just beyond the inception of cavitation was used as the flow. The corrected temperature was used as the temperature of the run.

There are many methods of displaying cavitation data in graphical form, and Stepanoff (p 266, *4*) and Church (p 83, *13*) have outlined several. The conventional methods consist in plotting pump efficiency vs Thoma's cavitation factor or static head at pump suction, and pump head vs Thoma's cavitation factor or static head at pump suction. These data were plotted in terms of pump head vs static head at pump suction.

The equations for reducing test data to pump head and static head at pump suction are set forth in Appendix B. The flow rates were ascertained by using the equations presented in Appendix A and the temperature multiplier values presented in Table 6.

Pump head vs static head at pump suction was plotted for each run and is presented in the Appendix as Figs. 3 through 7, inclusive, for the water tests, and in Figs. 8 through 16, inclusive, for the high-temperature alloy runs. A smooth curve was drawn in order to utilize as many of the data points of each test as seemed practicable.

Several criteria for the determination of cavitation inception are outlined by Stepanoff (p 264, *4*). The criterion used here involved identifying the value of the static head at pump suction at which a continued drop in pump head occurred. Three criterion-determining methods were investigated, employing:

1. the intersection of the tangent to the nearly horizontal portion of the curve with the tangent to the sloping portion of the curve,
2. the intersection of a horizontal line drawn through the lowest noncavitating pump-head data point with the sloping portion of the curve,
3. the intersection of a horizontal line drawn 2 ft below the lowest noncavitating pump-head data point with the sloping portion of the curve.

The maximum deviation among the three methods for the difference between corresponding water and alloy cavitation inception points was 0.6 ft for run No. 1. The second method was chosen in order to determine the cavitation inception point for each run and is illustrated in Fig. 3.

THE CORRELATION OF DATA FOR WATER AND NaK

The correlation consists in a comparison of the cavitation inception data obtained with high-temperature NaK with an estimated value for cavitation inception. The estimated value was obtained by adding the difference in the vapor pressures of the two liquids (water and NaK) to the cavitation inception value obtained with water at the same conditions of pump speed and liquid flow.

Table 1 identifies the pump operating conditions for each run and presents a comparison of the estimated value for cavitation inception with the experimental values for cavitation inception for each NaK run.

For run 1 (Table 1), the estimated cavitation inception value for NaK, 64.3 ft, was obtained by adding 19.2 ft (the difference between the vapor pressure of water and NaK for this run) to 45.1 ft (the cavitation inception value for water for this run). The experimentally determined cavitation inception value for NaK is 63.3 ft. Therefore, the estimate is high by 1 ft for run 1.

DISCUSSION

In this section, a coincidence of the largest differences between estimated and experimental cavitation inception for NaK with the largest difference between the vapor pressures of water and NaK will be pointed out, and the effect of temperature change on vapor pressure will be discussed.

The average difference (between the estimated and experimental values for cavitation inception by NaK) arising from the 138°F water-test estimates as presented in the last column of Table 1 was 3.9 ft, and the average difference arising from the 188°F water-test estimates was 1.5 ft. The average difference between the vapor pressures of corresponding water tests and high-temperature NaK tests was 36.4 ft for 138°F water and 20.1 ft for 188°F water. The largest difference between vapor pressures is associated with the larger average difference of 3.9 ft. Identical comments may be made for the 430 and 300 gpm runs. Whether this relationship can be deduced from flow considerations or from thermodynamic properties other than the vapor pressure of the alloy and of the water at 138 and at 188°F, or whether the fact is a coincidence, is not known to the author.

Figure 17 shows that a temperature change of 2°F changes the vapor pressure of 188°F water by 1 ft. From Fig. 19 it can be seen that a temperature change of 4.4°F effects a change of 1 ft in the vapor pressure of 1500°F NaK. The necessity for precise temperature measurement is readily apparent, and although much effort was expended to obtain satisfactory measurements, the precision required for identifying a change of 1 ft in vapor pressure (particularly for 1500°F NaK) cannot be guaranteed for the test. The equipment is gross, consisting of about 35 gal of alloy in about 1500 lb of Inconel and requiring a safety-shielded volume of about 1200 ft^3. The differences noted above are not easily subject to explanation.

CONCLUSIONS AND RECOMMENDATIONS

CONCLUSIONS

1. For the centrifugal pump under investigation, the static head at pump suction, in feet absolute, at cavitation inception was correlated for water and for 1500°F NaK on the basis of the differences of the vapor pressures of the two liquids. The difference between the vapor pressure of water and NaK, for the same conditions of pump speed and liquid flow, was added to the water-test cavitation inception value, and this estimate proved to be a good approximation to the experimental value found for cavitation inception with NaK.

2. The nine estimated values for cavitation inception by 1500°F NaK differ from the experimental values over a range of +1 ft to −4.9 ft. The differences yield a maximum average difference of 4.1 ft, which may be expressed as an average of 5% of the pump suction static head values at cavitation inception for the nine NaK runs.

3. It is suggested that, for the pump studied, cavitation inception with other liquid metals may be estimated on the basis of water-test cavitation inception and vapor pressure data. However, for other pumps and other liquids, similar experimental correlations should be obtained.

RECOMMENDATIONS

1. It is recommended that the temperatures of the liquids be more accurately determined in any future attempt to correlate the data for cavitation inception by a centrifugal pump, particularly if any of the liquids exhibit a steep slope of vapor pressure vs temperature.

2. It is also recommended that the use of smaller testing facilities be investigated.

BIBLIOGRAPHY

(*1*) W. B. Hall and T. I. M. Crofts, "The Use of Sodium and Sodium-Potassium Alloy as a Heat Transfer Media," *Atomics* **7**(8), 273, 290 (1956).

(*2*) J. M. Trummel, *Some Observations Made of Cavitating Sodium Flow in a Venturi*, ORNL CF-54-8-225 (Aug. 31, 1954).

(*3*) A. J. Stepanoff, "Propeller Pumps for Circulation of Molten Salt," *Refiner and Natural Gasoline Manufacturer* **19**(12), 74–76.

(*4*) A. J. Stepanoff, *Centrifugal and Axial Flow Pumps*, Wiley, New York, 1948.

(*5*) *Final Report, Development of Hermetically Sealed Centrifugal Pump Units for Liquid Metals*, Nuclear Power Section, Allis-Chalmers Manufacturing Co., Milwaukee, Wis., p 59–63 (June 30, 1953). Subcontract No. 56, under Contract No. W-31-109-ENG-52.

(*6*) H. C. Young and J. N. Simpson, ORNL CF-57-9-97 (Sept. 1957) (classified).

(*7*) H. J. Metz, personal communication.

(*8*) J. N. Simpson, personal communication.

(*9*) A. L. Southern, personal communication.

(*10*) J. H. Keenan and F. G. Keyes, *Thermodynamic Properties of Steam*, Wiley, New York, 1936.

(*11*) R. R. Miller, C. T. Ewing, R. S. Hartman, and H. B. Atkinson, Jr., *Quarterly Progress Report No. 3 in the Measurement of the Physical and Chemical Properties of the Sodium-Potassium Alloy*, Naval Research Laboratory Report No. C-3105, p 9–12 (April 1947).

(*12*) *Liquid Metals Handbook*, 3d ed., Sodium-NaK Supplement, Atomic Energy Commission and The Department of the Navy, GPO, Washington, (1955).

(*13*) A. H. Church, *Centrifugal Pumps and Blowers*, Wiley, New York, 1944.

APPENDIX A

LIST OF FIGURES

UNCLASSIFIED
ORNL-LR-DWG 30336

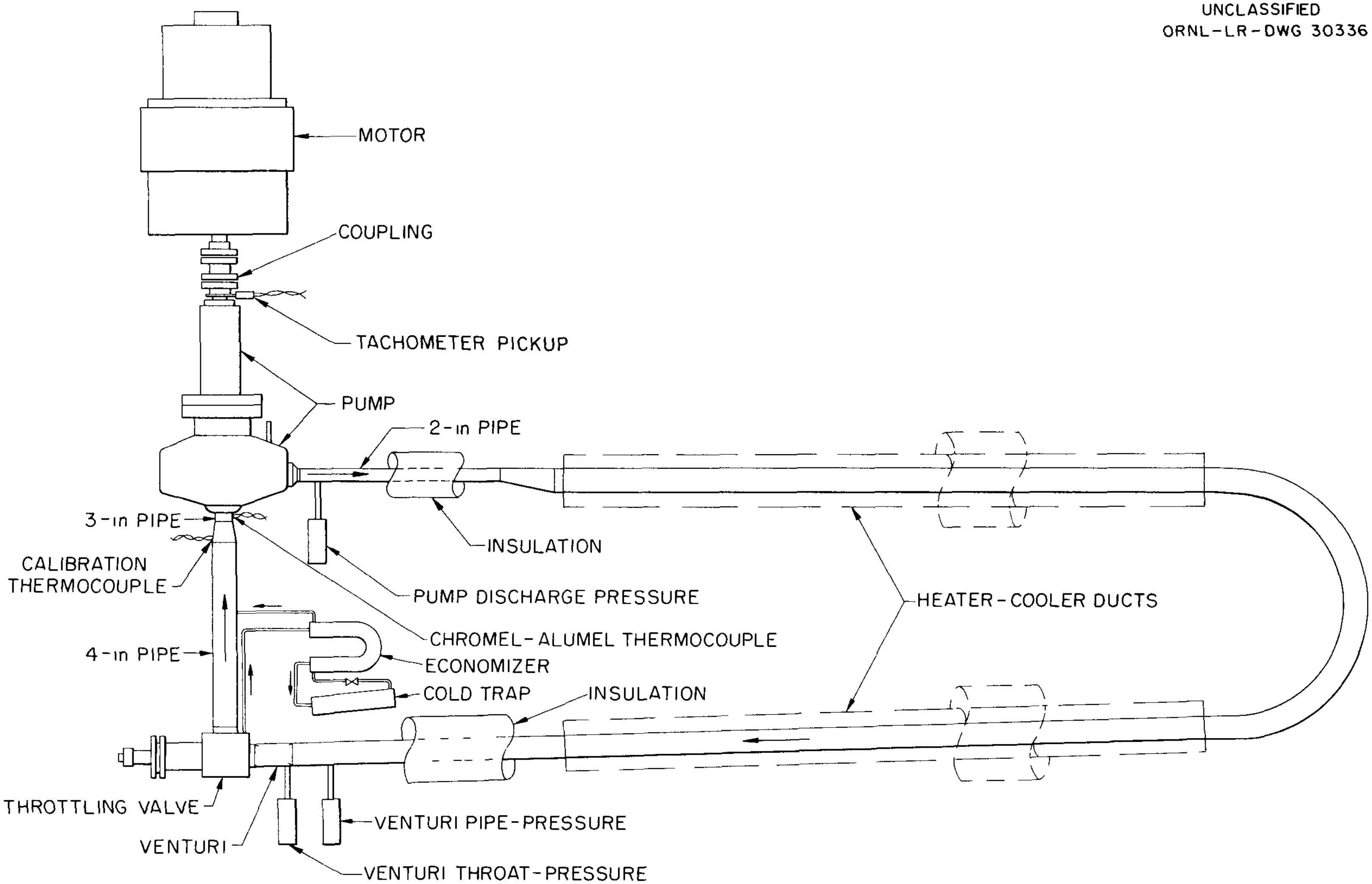

Fig. 1. Test Loop for Cavitation Inception Tests.

UNCLASSIFIED
ORNL-LR-DWG 33038

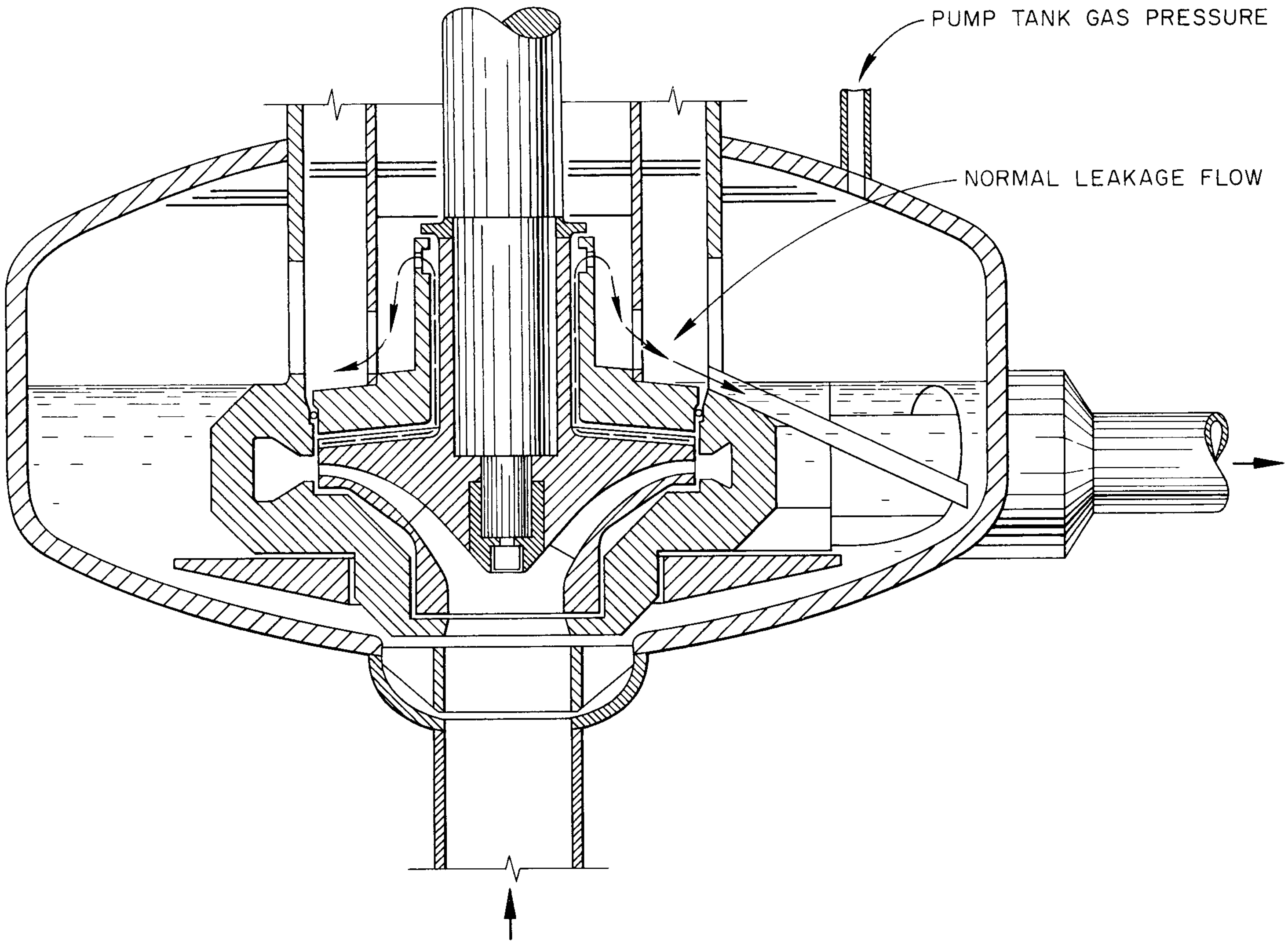

Fig. 2. Centrifugal Pump and Expansion Tank.

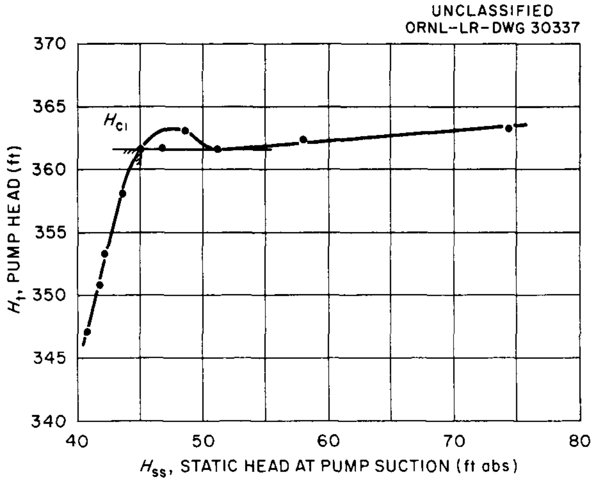

Fig. 3. Cavitation Inception Point for Water, Run 1. H_t vs H_{ss}, at 190°F, 3375 rpm, 300 gpm.

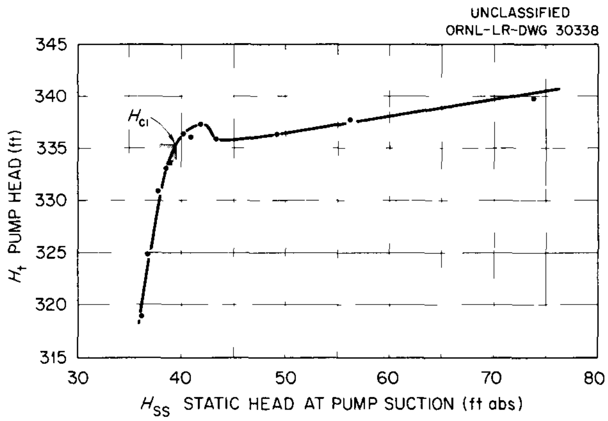

Fig. 4. Cavitation Inception Point for Water, Run 2. H_t vs H_{ss}, at 140°F, 3375 rpm, 430 gpm.

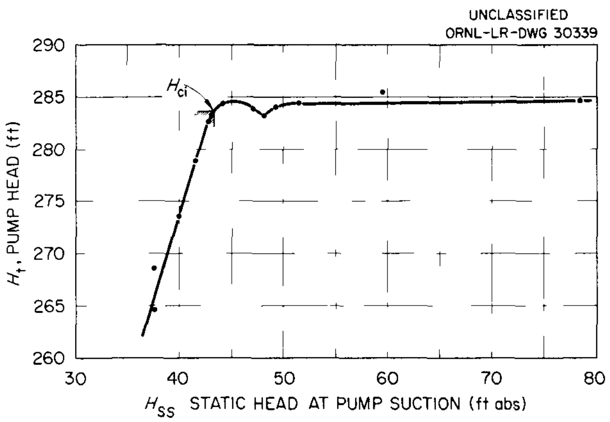

Fig. 5. Cavitation Inception Point for Water, Run 3. H_t vs H_{ss}, at 190°F, 3000 rpm, 300 gpm.

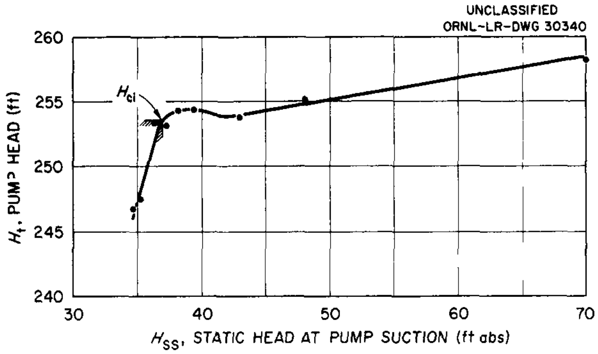

Fig. 6. Cavitation Inception Point for Water, Run 4. H_t vs H_{ss}, at 140°F, 3000 rpm, 430 gpm.

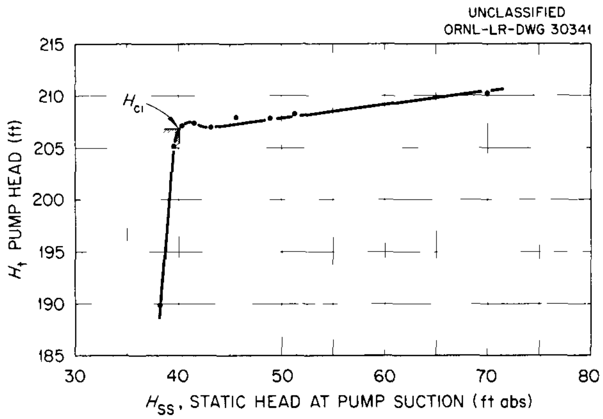

Fig. 7. Cavitation Inception Point for Water, Run 5. H_t vs H_{ss}, at 190°F, 2600 rpm, 300 gpm.

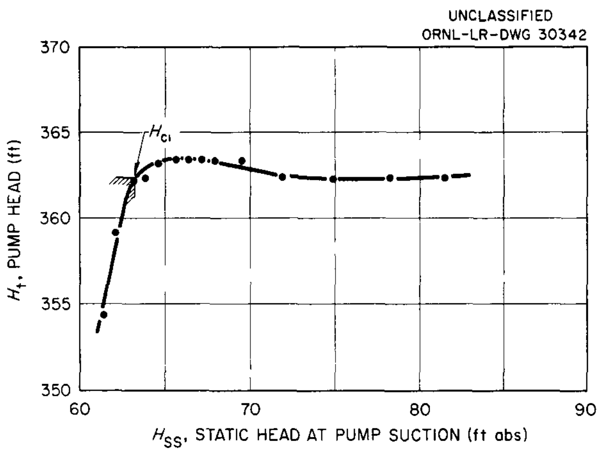

Fig. 8. Cavitation Inception Point for NaK, Run 1. H_t vs H_{ss}, at 1500°F, 3390 rpm, 300 gpm.

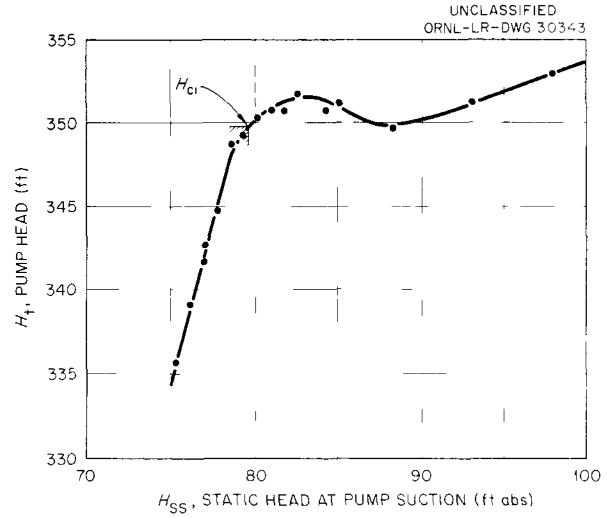

Fig. 9. Cavitation Inception Point for NaK, Run 2. H_t vs H_{ss}, at 1500°F, 3380 rpm, 430 gpm.

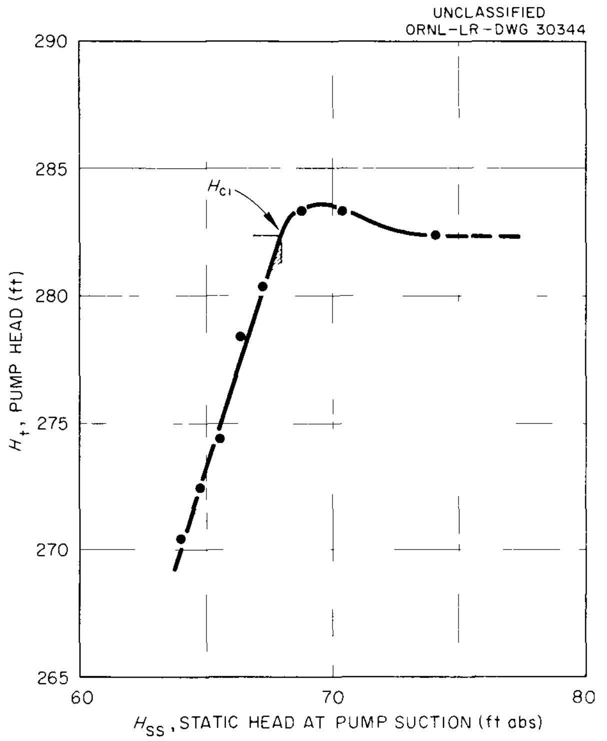

Fig. 10. Cavitation Inception Point for NaK, Run 3A. H_t vs H_{ss}, at 1500°F, 3018 rpm, 300 gpm.

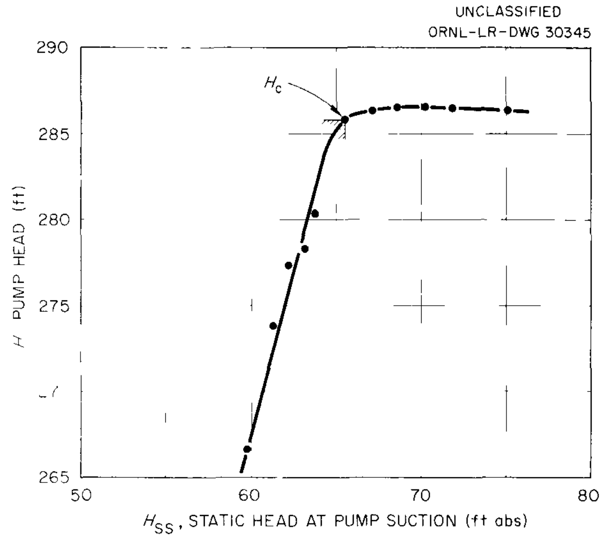

Fig. 11. Cavitation Inception Point for NaK, Run 3B. H_t vs H_{ss}, at 1500°F, 3030 rpm, 300 gpm.

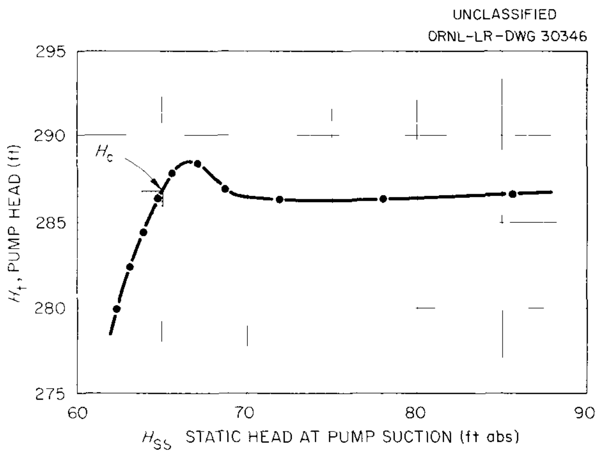

Fig. 12. Cavitation Inception Point for NaK, Run 3C. H_t vs H_{ss}, at 1500°F, 3030 rpm, 300 gpm.

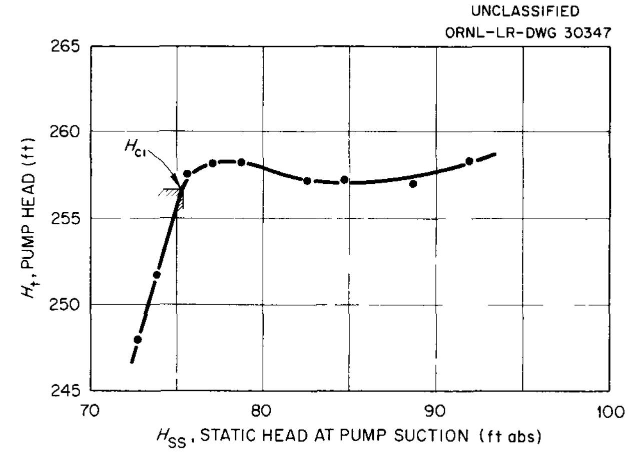

Fig. 13. Cavitation Inception Point for NaK, Run 4A. H_t vs H_{ss}, at 1500°F, 3000 rpm, 430 gpm.

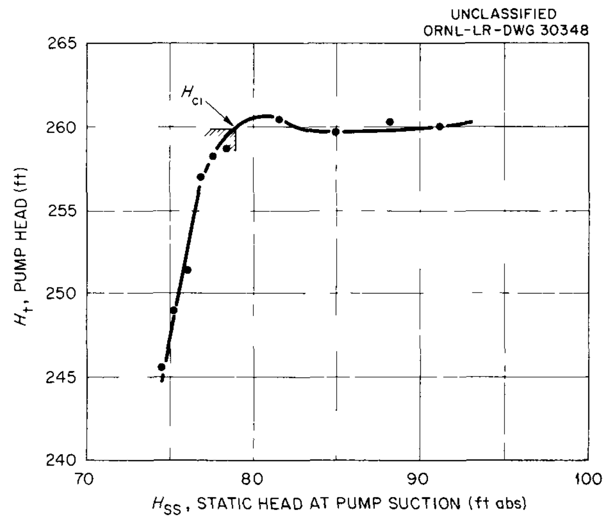

Fig. 14. Cavitation Inception Point for NaK, Run 4B. H_t vs H_{ss}, at 1500°F, 3000 rpm, 430 gpm.

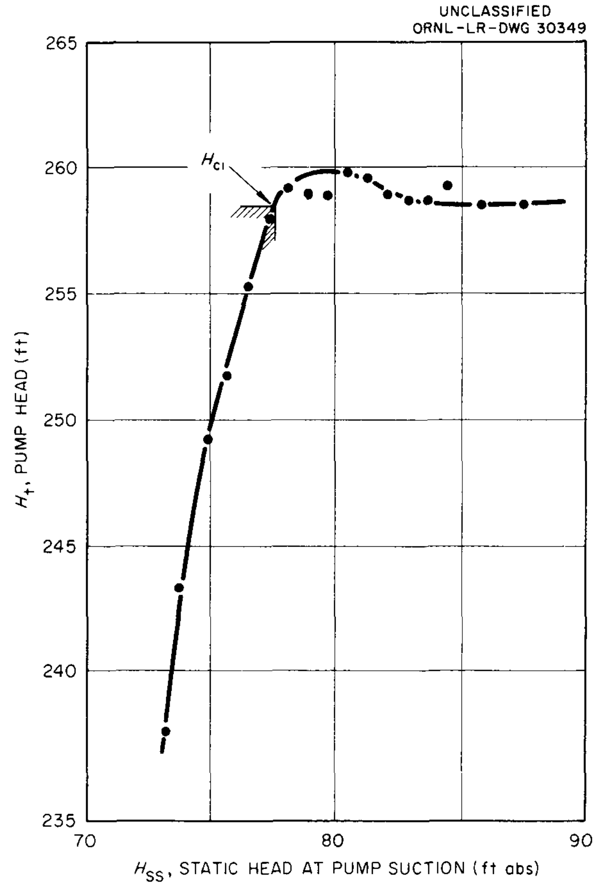

Fig. 15. Cavitation Inception Point for NaK, Run 4C. H_t vs H_{ss}, at 1500°F, 2985 rpm, 430 gpm.

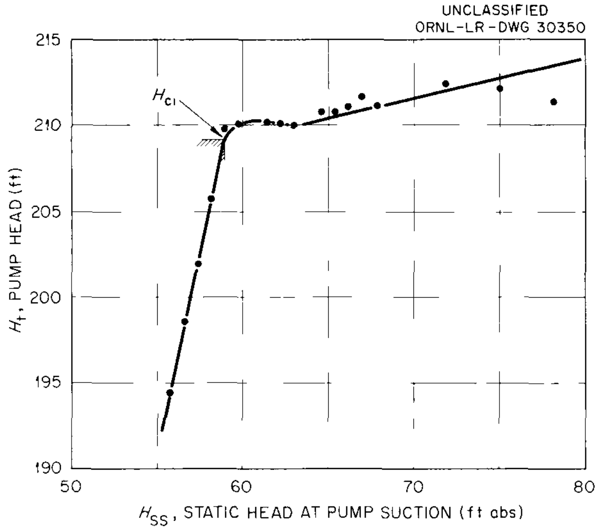

Fig. 16. Cavitation Inception Point for NaK, Run 5. H_t vs H_{ss}, at 1500°F, 2600 rpm, 300 gpm.

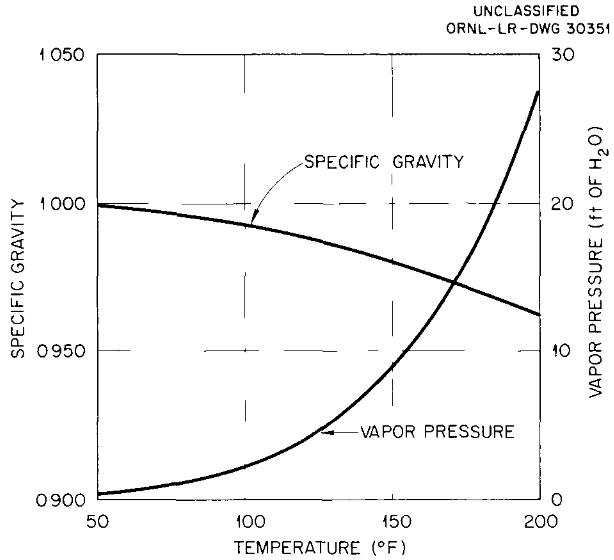

Fig. 17. Vapor Pressure and Specific Gravity of Water vs Temperature. See ref *10*.

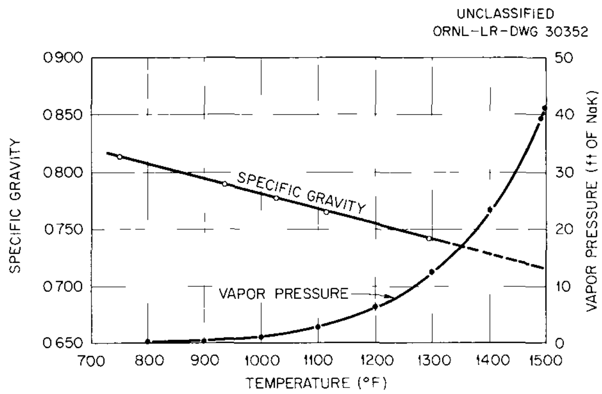

Fig. 18. Vapor Pressure (ref *11*) and Specific Gravity (ref *12*) of NaK (56 wt % Na) vs Temperature.

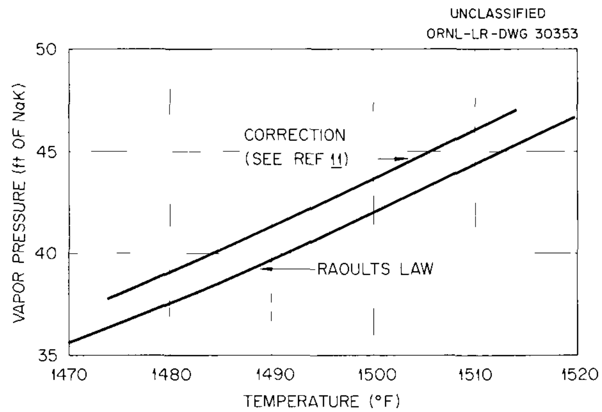

Fig. 19. Vapor Pressure of NaK (56 wt % Na) vs Temperature.

APPENDIX B

LIST OF TABLES

Table 1. Comparison of Water and NaK Data for Cavitation Inception by Centrifugal Pump

Water Tests						Sodium-Potassium Tests								
Run No.	N_{av} (rpm)	Q_{av} (gpm)	T (°F)	H_{ci} (ft abs)	H_{vp} (ft)	Run No.	N_{av} (rpm)	Q_{av} (gpm)	T (°F)	H_{vp} (ft)	H_{ci} (ft abs) Estimated	H_{ci} (ft abs) Alloy Test	Difference (ft)	Difference (%)
1	3375	306	188	45.1	21.3	1	3390	308	1490	40.5	64.3	63.3	+1.0	+1.6
2	3374	436	138	39.5	6.4	2	3383	435	1501	43.0	76.1	79.8	−3.7	−4.7
3	3003	306	188	43.2	21.3	3A	3018	310	1502	43.2	65.1	68.0	−2.9	−4.3
						3B	3030	305	1497	42.1	64.0	65.5	−1.5	−2.3
						3C	3047	307	1500	42.7	64.6	65.0	−0.4	−0.6
4	2999	436	138	37.0	6.4	4A	3000	432	1493	41.2	71.8	75.4	−3.6	−4.8
						4B	3000	432	1503	43.5	74.1	79.0	−4.9	−6.2
						4C	2985	435	1503	43.5	74.1	77.6	−3.5	−4.5
5	2603	304	188	40.2	21.3	5	2601	303	1481	38.5	57.4	59.0	−1.6	−2.7

Table 2. Cavitation Inception Data for Water Tests

	N (rpm)	T (°F)	P_d (psig)	P_{pt} (psig)	P_p (psig)	P_t (psig)
Run 1	3375	189	165.8	16.7	167.9	149.4
Date 1-28-57	3371	189	158.6	9.9	160.6	142.4
Bar. 29.30 in. Hg	3377	190	155.4	7.0	157.7	139.3
	3377	190	155.0	6.0	157.2	138.8
	3375	190	153.5	5.1	155.5	137.2
	3375	190	152.9	4.5	154.9	136.8
	3378	190	150.8	3.9	152.9	134.8
	3372	190	148.2	3.3	150.4	132.3
	3374	190	147.0	3.1	148.9	130.8
	3377	190	145.0	2.7	146.8	128.7
Run 2	3372	141	154.0	17.0	159.2	121.3
Date 12-27-56	3373	140	145.7	9.5	150.8	112.5
Bar. 29.37 in. Hg	3375	138.5	142.0	6.5	147.3	109.4
	3372	140	139.2	4.0	144.4	106.3
	3374	140	139.3	3.4	144.5	106.4
	3377	140	138.4	3.0	143.5	104.8
	3373	140	138.2	2.7	143.1	105.0
	3375	140	136.2	2.0	140.9	102.9
	3371	140	134.9	1.6	139.4	101.6
	3376	140	131.8	1.2	136.5	98.7
	3376	140	129.0	1.0	133.9	95.8

Table 2 (continued)

	N (rpm)	T (°F)	P_d (psig)	P_{pt} (psig)	P_p (psig)	P_t (psig)
Run 3	3000	190	134.0	18.0	136.2	117.9
Date 1-30-57	3003	188	129.9	10.5	128.8	110.5
Bar. 29.36 in. Hg	3005	188	123.0	7.1	124.9	116.7
	3000	189	122.0	6.2	123.9	105.5
	3000	190	121.1	5.7	123.2	104.9
	3004	190	121.0	5.3	123.0	104.6
	3004	191	120.0	4.1	122.1	103.9
	3002	191	118.7	3.5	120.8	102.4
	3005	190	116.6	3.0	119.1	100.7
	3001	190	113.7	2.3	116.0	97.6
	3008	190	110.6	1.3	113.0	94.7
	3004	190	109.0	1.3	111.1	92.6
Run 4	2999	140	117.8	15.6	122.7	84.8
Date 12-29-56	3001	140	106.9	6.2	111.8	73.6
Bar. 29.02 in. Hg	3002	140	104.2	4.0	108.8	70.7
	2999	141	103.0	2.5	107.3	69.2
	3001	141	102.5	2.0	106.8	68.5
	2993	141	97.7	0.5	102.8	64.3
	2999	140	101.3	1.3	105.1	67.2
	2999	140	98.3	0.8	103.0	65.0
	3001	140	102.3	1.6	106.3	68.5
Run 5	2607	190	99.7	14.8	102.1	84.0
Date 1-4-57	2600	190	91.2	7.0	93.9	76.0
Bar. 29.28 in. Hg	2602	190	90.0	6.0	92.4	74.2
	2602	190	88.6	4.6	91.0	73.0
	2603	190	87.1	3.5	89.7	71.5
	2603	189	86.7	2.9	89.0	71.0
	2605	190	86.2	2.4	89.0	70.5
	2599	190	85.0	2.1	87.2	69.1
	2604	192	78.0	1.5	80.4	62.4
	2607	190	99.7	14.8	102.1	84.0
	2600	190	91.2	7.0	93.9	76.0
	2602	190	90.0	6.0	92.4	74.2
	2602	190	88.6	4.6	91.0	73.0
	2603	190	87.1	3.5	89.7	71.5
	2603	189	86.7	2.9	89.0	71.0
	2605	190	86.2	2.4	89.0	70.5
	2599	190	85.0	2.1	87.2	69.1
	2604	192	78.0	1.5	80.4	62.4

Table 3. Computations of Cavitation Inception Data Obtained with Water

Run 1												
P_d (psig)	165.8	158.6	155.4	155.0	153.5	152.9	150.8	148.2	147.0	145.0		
P_{pt} (psig)	16.7	9.9	7.0	6.0	5.1	4.5	3.9	3.3	3.1	2.7		
$P_d - P_{pt}$ (psi)	149.1	148.7	148.4	149.0	148.4	148.4	146.9	144.9	143.9	142.3		
$\frac{2.31}{\text{sp gr}}(P_d - P_{pt})$ (ft)	356.0	355.2	354.5	355.9	354.5	354.5	350.9	346.1	343.7	339.9		
$C + \Delta V^2/2g$ (ft)	7.2	7.2	7.2	7.2	7.2	7.2	7.2	7.2	7.2	7.2		
H_t (ft)	363.2	362.4	361.7	363.1	361.7	361.7	358.1	353.3	350.9	347.1		
$\frac{2.31}{\text{sp gr}}(P_{pt})$ (ft)	40.0	23.6	16.7	14.3	12.2	10.7	9.3	7.9	7.4	6.4		
Bar. (ft)	34.4	34.4	34.4	34.4	34.4	34.4	34.4	34.4	34.4	34.4		
H_{ss} (ft abs)	74.4	58.0	51.1	48.7	46.6	45.1	43.7	42.3	41.8	40.8		
ΔP_v (psi)	18.5	18.4	18.4	18.4	18.3	18.1	18.1	18.1	18.1	18.1		
Run 2												
P_d (psig)	154.0	145.7	142.0	139.2	139.3	138.4	138.2	136.2	134.9	131.8	129.0	
P_{pt} (psig)	17.0	9.5	6.5	4.0	3.4	3.0	2.7	2.0	1.6	1.2	1.0	
$P_d - P_{pt}$ (psi)	137.0	136.2	135.5	135.2	135.9	135.4	135.5	134.2	133.3	130.6	128.0	
$\frac{2.31}{\text{sp gr}}(P_d - P_{pt})$ (ft)	322.0	320.0	318.5	318.0	319.5	318.2	318.5	315.2	313.0	307.0	301.0	
$C + \Delta V^2/2g$ (ft)	17.9	17.9	17.9	17.9	17.9	17.9	17.9	17.9	17.9	17.9	17.9	
H_t (ft)	339.9	337.9	336.4	335.9	337.4	336.1	336.4	333.1	330.9	324.9	318.9	
$\frac{2.31}{\text{sp gr}}(P_{pt})$ (ft)	39.9	22.3	15.3	9.4	8.0	7.0	6.3	4.7	3.9	2.9	2.3	
Bar. (ft)	33.9	33.9	33.9	33.9	33.9	33.9	33.9	33.9	33.9	33.9	33.9	
H_{ss} (ft abs)	73.8	56.2	49.2	43.3	41.9	40.9	40.2	38.6	37.8	36.8	36.2	
ΔP_v (psi)	37.9	38.3	37.9	38.1	38.1	38.7	38.1	38.0	37.8	37.8	38.1	
Run 3												
P_d (psig)	134.0	126.9	123.0	122.0	121.1	121.0	120.0	118.7	116.6	113.7	110.6	109.0
P_{pt} (psig)	18.0	10.5	7.1	6.2	5.7	5.3	4.1	3.5	3.0	2.3	1.3	1.3
$P_d - P_{pt}$ (psi)	116.0	116.4	115.9	115.8	115.4	115.7	115.9	115.2	113.6	111.4	109.3	107.7
$\frac{2.31}{\text{sp gr}}(P_d - P_{pt})$ (ft)	277.4	278.3	277.2	276.9	276.0	276.7	277.2	275.5	271.7	266.4	261.4	257.5
$C + \Delta V^2/2g$ (ft)	7.2	7.2	7.2	7.2	7.2	7.2	7.2	7.2	7.2	7.2	7.2	7.2
H_t (ft)	284.6	285.5	284.4	284.1	283.2	283.9	284.4	282.7	278.9	273.6	268.6	264.7
$\frac{2.31}{\text{sp gr}}(P_{pt})$ (ft)	43.0	25.1	17.0	14.8	13.6	12.7	9.8	8.4	7.2	5.5	3.1	3.1

Table 3 (continued)

Run 3												
Bar. (ft)	34.5	34.5	34.5	34.5	34.5	34.5	34.5	34.5	34.5	34.5	34.5	34.5
H_{ss} (ft abs)	77.5	59.6	51.5	49.3	48.1	47.2	44.3	42.9	41.7	40.0	37.6	37.6
ΔP_v (psi)	18.3	18.3	18.2	18.4	18.3	18.4	18.2	18.4	18.4	18.4	18.3	18.5
Run 4												
P_d (psig)	117.8	106.9	104.2	103.0	102.5	97.7	101.3	98.3	102.3			
P_{pt} (psig)	15.6	6.2	4.0	2.5	2.0	0.5	1.3	0.8	1.6			
$P_d - P_{pt}$ (psi)	102.2	100.7	100.2	100.5	100.5	97.2	100.0	97.5	100.7			
$\frac{2.31}{\text{sp gr}}(P_d - P_{pt})$ (ft)	240.0	236.8	235.5	236.0	236.0	228.4	235.0	229.1	236.8			
$C + \Delta V^2/2g$ (ft)	18.4	18.4	18.4	18.4	18.4	18.4	18.4	18.4	18.4			
H_t (ft abs)	258.4	255.2	253.9	254.4	254.4	246.8	253.4	247.5	253.2			
$\frac{2.31}{\text{sp gr}}(P_{pt})$ (ft)	36.7	14.6	9.4	5.9	4.7	1.2	2.9	1.8	3.8			
Bar. (ft)	33.5	33.5	33.5	33.5	33.5	33.5	33.5	33.5	33.5			
H_{ss} (ft abs)	70.2	48.1	42.9	39.4	38.2	34.7	36.4	35.3	37.3			
ΔP_v (psi)	37.9	38.2	38.1	38.1	38.3	38.5	37.9	38.0	37.8			
Run 5												
P_d (psig)	99.7	91.2	90.0	88.6	87.1	86.7	86.2	85.0	78.0			
P_{pt} (psig)	14.8	7.0	6.0	4.6	3.5	2.9	2.4	2.1	1.5			
$P_d - P_{pt}$ (psi)	84.9	84.2	84.0	84.0	83.6	83.8	83.8	82.9	76.5			
$\frac{2.31}{\text{sp gr}}(P_d - P_t)$ (ft)	203.0	201.1	200.7	200.7	199.8	200.2	200.2	198.0	182.7			
$C + \Delta V^2/2g$ (ft)	7.2	7.2	7.2	7.2	7.2	7.2	7.2	7.2	7.2			
H_t (ft)	210.2	208.3	207.9	207.9	207.0	207.4	207.4	205.2	189.9			
$\frac{2.31}{\text{sp gr}}(P_{pt})$ (ft)	35.3	16.7	14.3	11.0	8.4	6.9	5.7	5.0	3.6			
Bar. (ft)	34.7	34.7	34.7	34.7	34.7	34.7	34.7	34.7	34.7			
H_{ss} (ft abs)	70.0	51.4	49.0	45.7	43.1	41.6	40.4	39.7	38.3			
ΔP_v (psi)	18.1	17.9	18.2	18.0	18.2	18.0	18.5	18.1	18.0			

Table 4. Cavitation Inception Data for NaK Tests

	N (rpm)	T (°F)	P_d (psig)	P_{pt} (psig)	P_p (psig)	P_t (psig)
Run 1	3390	1500	121.0	11.0	124.2	110.6
Date 10-18-57	3390	1498	120.0	10.0	123.1	109.6
Bar. 27.17 in. Hg	3390	1498	119.0	9.0	122.1	108.6
	3390	1497	118.0	8.0	121.4	108.0
	3390	1497	117.6	7.2	120.7	107.3
	3390	1497	117.1	6.7	120.3	107.0
	3390	1497	116.8	6.5	120.0	106.4
	3390	1497	116.5	6.2	119.8	106.4
	3390	1497	116.3	6.0	119.6	106.2
	3390	1497	116.0	5.7	119.4	106.0
	3390	1497	115.6	5.5	118.9	105.6
	3390	1497	115.0	5.2	118.4	105.2
	3390	1497	114.0	4.9	117.4	104.2
	3390	1497	113.0	4.7	116.2	103.2
Run 2	3382	1508	117.0	16.0	122.7	96.9
Date 10-26-57	3385	1508	115.2	14.5	121.0	94.3
Bar. 29.15 in. Hg	3382	1508	113.1	13.0	119.3	92.6
	3383	1508	112.5	12.0	118.3	91.9
	3382	1508	112.1	11.7	118.0	91.6
	3377	1508	111.8	11.2	117.6	91.2
	3382	1508	111.3	11.0	117.4	90.9
	3378	1508	111.1	10.7	117.2	90.6
	3381	1508	110.7	10.5	116.7	90.2
	3384	1508	110.2	10.2	116.4	89.8
	3387	1508	109.7	10.0	115.6	89.2
	3391	1508	108.2	9.7	113.9	88.2
	3378	1508	107.3	9.5	112.9	87.2
	3382	1508	107.1	9.5	112.6	87.0
	3388	1508	106.0	9.2	111.6	86.2
	3389	1508	104.7	9.0	110.4	85.3
Run 3A	3018	1510	93.0	8.6	96.9	83.5
Date 10-17-57	3018	1510	92.2	7.5	96.3	82.8
Bar. 29.05 in. Hg	3018	1510	91.7	7.0	95.7	82.2
	3018	1510	90.3	6.5	94.4	81.0
	3018	1510	89.3	6.2	93.5	80.4
	3018	1510	88.0	6.0	92.2	79.2
	3018	1510	87.0	5.7	91.1	78.3
	3018	1510	86.0	5.5	90.2	77.2
Run 3B	3030	1504	94.9	9.0	98.8	85.7
Date 10-17-57	3030	1504	94.0	8.0	97.8	84.8
Bar. 29.05 in. Hg	3030	1504	93.5	7.5	97.4	84.3
	3030	1504	93.0	7.0	97.0	83.9
	3030	1504	92.5	6.5	96.5	83.3
	3030	1504	91.8	6.0	95.7	82.6

Table 4 (continued)

	N (rpm)	T (°F)	P_d (psig)	P_{pt} (psig)	P_p (psig)	P_t (psig)
Run 3B	3030	1504	89.8	5.5	93.8	81.0
Date 10-17-57	3030	1504	88.6	5.2	92.7	79.9
Bar. 29.05 in. Hg	3030	1504	87.4	5.0	91.4	78.8
	3030	1504	86.7	4.7	90.5	78.1
	3030	1504	84.0	4.2	87.8	75.6
Run 3C	3030	1500	98.3	12.2	102.2	88.8
Date 10-18-57	3030	1507	96.0	9.8	100.1	87.0
Bar. 29.17 in. Hg	3034	1507	94.0	8.0	98.1	85.0
	3052	1507	93.1	7.0	97.2	84.2
	3042	1507	93.0	6.5	96.9	83.9
	3055	1507	92.1	6.0	96.2	83.2
	3055	1507	91.6	5.7	95.6	82.6
	3055	1507	90.8	5.5	94.8	81.8
	3055	1507	89.9	5.2	94.0	81.1
	3058	1507	88.7	5.0	92.7	80.0
Run 4A	3000	1501	87.1	14.1	93.9	67.8
Date 10-11-57	3000	1501	85.7	13.1	92.0	65.8
Bar. 29.3 in. Hg	3000	1501	84.5	11.8	90.8	64.7
	3000	1499	83.9	11.2	90.0	63.8
	3000	1500	82.9	10.0	89.0	63.0
	3000	1500	82.4	9.5	88.0	62.0
	3000	1500	81.4	9.0	87.2	61.3
	3000	1500	79.4	8.5	85.6	60.0
	3000	1500	77.8	8.1	83.0	57.0
Run 4B	3000	1510	87.6	13.9	94.3	67.6
Date 10-18-57	3000	1510	86.6	13.0	93.1	66.5
Bar. 29.17 in. Hg	3000	1510	85.4	12.0	91.8	65.4
	3000	1510	84.6	10.9	90.8	64.3
	3000	1510	83.1	10.0	89.3	62.8
	3000	1510	82.7	9.7	88.7	62.4
	3000	1510	81.9	9.5	87.9	62.0
	3000	1510	80.0	9.2	86.4	60.0
	3000	1510	79.0	9.0	85.4	59.3
	3000	1510	77.7	8.7	83.3	57.5
Run 4C	2985	1510	85.5	12.6	91.6	65.1
Date 10-18-57	2985	1510	85.0	12.1	90.9	64.5
Bar. 29.17 in. Hg	2985	1510	84.8	11.7	90.6	64.0
	2985	1510	84.4	11.5	90.4	63.8
	2985	1510	84.1	11.2	90.1	63.6
	2985	1510	84.0	11.0	89.8	63.3
	2985	1510	83.9	10.7	89.6	63.0
	2985	1510	83.7	10.5	89.4	62.9
	2985	1510	83.2	10.2	89.1	62.4

Table 4 (continued)

	N (rpm)	T (°F)	P_d (psig)	P_{pt} (psig)	P_p (psig)	P_t (psig)
Run 4C	2985	1510	83.0	10.0	88.6	62.2
Date 10-18-57	2985	1510	82.8	9.7	88.3	61.9
Bar. 29.17 in. Hg	2985	1510	82.2	9.5	87.8	61.5
	2985	1510	81.1	9.2	86.6	60.5
	2985	1510	79.6	9.0	85.2	59.6
	2985	1510	78.6	8.7	84.4	59.0
	2985	1510	76.5	8.4	82.0	57.2
	2985	1510	74.5	8.2	80.9	55.7
Run 5	2600	1487	72.4	9.9	75.0	62.5
Date 10-18-57	2600	1487	71.7	9.0	74.6	61.8
Bar. 29.18 in. Hg	2600	1487	70.8	8.0	73.7	60.8
	2600	1487	69.1	6.7	72.2	59.4
	2600	1487	69.0	6.5	72.0	59.2
	2603	1486	68.6	6.2	71.6	58.7
	2603	1486	68.2	6.0	71.3	58.6
	2603	1486	68.0	5.7	71.0	58.4
	2603	1486	67.0	5.2	70.1	57.3
	2603	1486	66.8	5.0	69.8	57.0
	2603	1488	66.6	4.7	69.6	56.8
	2603	1488	66.0	4.2	69.1	56.0
	2603	1488	65.7	4.0	69.0	55.7
	2603	1488	64.2	3.7	67.7	54.5
	2603	1488	62.8	3.5	65.8	53.2
	2603	1488	61.5	3.2	64.5	52.1
	2603	1488	60.0	3.0	63.0	50.8

Table 5. Computations of Cavitation Inception Data Obtained with NaK

Run 1																
P_{dc} (psig)	119.6	118.6	117.6	116.6	116.2	115.7	115.4	115.1	114.9	114.6	114.2	113.6	112.6	111.6		
P_{pt} (psig)	11.0	10.0	9.0	8.0	7.2	6.7	6.5	6.2	6.0	5.7	5.5	5.2	4.9	4.7		
$P_{dc} - P_{pt}$ (psi)	108.6	108.6	108.6	108.6	109.0	109.0	108.9	108.9	108.9	108.9	108.7	108.4	107.7	106.9		
$\frac{2.31}{\text{sp gr}}(P_{dc} - P_{pt})$ (ft)	350.0	350.0	350.0	350.0	351.0	351.0	351.0	351.0	351.0	351.0	350.2	349.9	347.0	342.0		
$C + \Delta V^2/2g$ (ft)	12.4	12.4	12.4	12.4	12.4	12.4	12.4	12.4	12.4	12.4	12.4	12.4	12.4	12.4		
H_t (ft)	362.4	362.4	362.4	362.4	363.4	363.4	363.4	363.4	363.4	363.4	363.4	362.3	359.4	354.4		
$\frac{2.31}{\text{sp gr}}(P_{pt})$ (ft)	35.4	32.2	29.0	25.8	23.4	21.8	21.0	20.2	19.5	18.5	17.7	16.9	16.0	15.3		
Bar. (ft)	46.2	46.2	46.2	46.2	46.2	46.2	46.2	46.2	46.2	46.2	46.2	46.2	46.2	46.2		
H_{ss} (ft abs)	81.6	78.4	75.2	72.0	69.6	68.0	67.2	66.4	65.7	64.7	63.9	63.1	62.2	61.5		
ΔP_{vc} (psi)	13.2	13.1	13.1	13.0	13.0	12.9	13.2	13.1	13.1	13.1	13.0	12.9	12.9	12.7		
Run 2																
P_{dc} (psig)	117.0	115.2	113.1	112.5	112.1	111.8	111.3	111.1	110.7	110.2	109.7	108.2	107.3	107.1	106.0	104.7
P_{pt} (psig)	16.0	14.5	13.0	12.0	11.7	11.2	11.0	10.7	10.5	10.2	10.0	9.7	9.5	9.5	9.2	9.0
$P_{dc} - P_{pt}$ (psi)	101.0	100.7	100.1	100.5	100.4	100.6	100.3	100.4	100.2	100.0	99.7	98.5	97.8	97.6	96.8	95.7
$\frac{2.31}{\text{sp gr}}(P_{dc} - P_{pt})$ (ft)	327.2	326.5	324.0	325.5	325.0	326.0	325.0	325.0	324.6	323.5	323.0	319.0	317.0	316.0	313.5	310.0
$C + \Delta V^2/2g$ (ft)	25.8	25.8	25.8	25.8	25.8	25.8	25.8	25.8	25.8	25.8	25.8	25.8	25.8	25.8	25.8	25.8
H_t (ft)	353.0	352.3	349.8	351.3	350.8	351.8	350.8	350.8	350.4	349.3	348.8	344.8	342.8	341.8	339.3	335.8
$\frac{2.31}{\text{sp gr}}(P_{pt})$ (ft)	51.8	47.0	42.1	38.9	38.1	36.4	35.6	34.8	34.0	33.2	32.4	31.6	30.8	30.8	30.0	29.2
Bar. (ft)	46.3	46.3	46.3	46.3	46.3	46.3	46.3	46.3	46.3	46.3	46.3	46.3	46.3	46.3	46.3	46.3
H_{ss} (ft abs)	98.1	93.3	88.4	85.2	84.4	82.7	81.9	81.1	80.3	79.5	78.7	77.9	77.1	77.1	76.3	75.5
ΔP_{vc} (psi)	25.4	26.3	26.4	26.1	26.1	26.1	26.2	26.3	26.2	26.3	26.1	25.4	25.4	25.3	25.1	24.9

Table 5 (continued)

Run 3A											
P_{dc} (psig)	91.9	91.1	90.6	89.2	88.2	87.0	86.0	85.0			
P_{pt} (psig)	8.6	7.5	7.0	6.5	6.2	6.0	5.7	5.5			
$P_{dc} - P_{pt}$ (psi)	83.3	83.6	83.6	82.7	82.0	81.0	80.3	79.5			
$\frac{2.31}{\text{sp gr}}(P_{dc} - P_{pt})$ (ft)	270.0	271.0	271.0	268.0	266.0	262.0	260.0	258.0			
$C + \Delta V^2/2g$ (ft)	12.4	12.4	12.4	12.4	12.4	12.4	12.4	12.4			
H_t (ft)	282.4	283.4	283.4	280.4	278.4	274.4	272.4	270.4			
$\frac{2.31}{\text{sp gr}}(P_{pt})$ (ft)	28.0	24.3	22.7	21.0	20.2	19.5	18.7	17.8			
Bar. (ft)	46.1	46.1	46.1	46.1	46.1	46.1	46.1	46.1			
H_{ss} (ft abs)	74.1	70.4	68.8	67.1	66.3	65.6	64.8	63.9			
ΔP_{vc} (psi)	13.2	13.4	13.3	13.2	12.9	12.8	12.6	12.8			
Run 3B											
P_{dc} (psig)	93.8	92.9	92.4	91.9	91.4	90.7	88.7	87.5	86.4	85.7	83.0
P_{pt} (psig)	9.0	8.0	7.5	7.0	6.5	6.0	5.5	5.2	5.0	4.7	4.2
$P_{dc} - P_{pt}$ (psi)	84.8	84.9	84.9	84.9	84.9	84.7	83.2	82.3	81.4	81.0	78.8
$\frac{2.31}{\text{sp gr}}(P_{dc} - P_{pt})$ (ft)	274.0	274.2	274.2	274.2	274.2	273.5	269.0	266.0	263.0	261.5	254.0
$C + \Delta V^2/2g$ (ft)	12.4	12.4	12.4	12.4	12.4	12.4	12.4	12.4	12.4	12.4	12.4
H_t (ft)	286.4	286.6	286.6	286.6	286.6	285.9	281.4	278.4	275.4	273.9	266.4
$\frac{2.31}{\text{sp gr}}(P_{pt})$ (ft)	29.1	25.8	24.2	22.6	21.0	19.4	17.8	17.0	16.2	15.4	13.7
Bar. (ft)	46.1	46.1	46.1	46.1	46.1	46.1	46.1	46.1	46.1	46.1	46.1
H_{ss} (ft abs)	75.2	71.9	70.3	68.7	67.1	65.5	63.9	63.1	62.3	61.5	59.8
ΔP_{vc} (psi)	12.9	12.8	12.9	12.9	13.0	13.0	12.6	12.6	12.4	12.2	12.1

Table 5 (continued)

Run 3C										
P_{dc} (psig)	97.1	94.8	92.9	92.0	91.9	91.0	90.5	89.7	88.8	87.6
P_{pt} (psig)	12.2	9.8	8.0	7.0	6.5	6.0	5.7	5.5	5.2	5.0
$P_{dc} - P_{pt}$ (psi)	84.9	85.0	84.9	85.0	85.4	85.0	84.8	84.2	83.6	82.6
$\frac{2.31}{\text{sp gr}}(P_{dc} - P_{pt})$ (ft)	274.0	274.5	274.2	274.7	276.0	274.7	273.9	272.0	270.0	267.5
$C + \Delta V^2/2g$ (ft)	12.4	12.4	12.4	12.4	12.4	12.4	12.4	12.4	12.4	12.4
H_t (ft)	286.4	286.9	286.6	287.1	288.4	287.1	286.3	284.4	282.4	279.9
$\frac{2.31}{\text{sp gr}}(P_{pt})$ (ft)	39.6	31.8	25.8	22.6	21.0	19.4	18.6	17.8	17.0	16.2
Bar. (ft)	46.2	46.2	46.2	46.2	46.2	46.2	46.2	46.2	46.2	46.2
H_{ss} (ft abs)	85.8	78.0	72.0	68.8	67.2	65.6	64.8	64.0	63.2	62.4
ΔP_{vc} (psi)	13.1	12.9	12.9	12.9	12.9	12.8	12.9	13.0	12.7	11.6
Run 4A										
P_{dc} (psig)	86.1	84.7	83.5	82.9	81.9	81.4	80.4	78.5	76.9	
P_{pt} (psig)	14.1	13.1	11.8	11.2	10.0	9.5	9.0	8.5	8.1	
$P_{dc} - P_{pt}$ (psi)	72.0	71.6	71.7	71.7	71.9	71.9	71.4	70.0	68.8	
$\frac{2.31}{\text{sp gr}}(P_{dc} - P_{pt})$ (ft)	232.5	231.2	231.4	231.5	232.3	232.3	230.8	226.0	222.0	
$C + \Delta V^2/2g$ (ft)	25.8	25.8	25.8	25.8	25.8	25.8	25.8	25.8	25.8	
H_t (ft)	258.3	257.0	257.2	257.3	258.1	258.1	256.6	251.8	247.8	
$\frac{2.31}{\text{sp gr}}(P_{pt})$ (ft)	45.4	42.2	38.2	36.1	32.2	30.6	29.0	27.4	26.3	
Bar. (ft)	46.5	46.5	46.5	46.5	46.5	46.5	46.5	46.5	46.5	
H_{ss} (ft abs)	91.9	88.7	84.7	82.6	78.7	77.1	75.5	73.9	72.8	
ΔP_{vc} (psi)	25.8	25.9	25.8	26.0	25.8	25.8	25.6	25.3	25.6	

Table 5 (continued)

Run 4B

P_{dc} (psig)	86.6	85.6	84.4	83.6	82.1	81.7	81.0	79.1	78.1	76.8
P_{pt} (psig)	13.9	13.0	12.0	10.9	10.0	9.7	9.5	9.2	9.0	8.7
$P_{dc} - P_{pt}$ (psi)	72.7	72.6	72.4	72.7	72.1	72.0	71.5	69.9	69.1	68.5
$\frac{2.31}{sp\ gr}(P_{dc}-P_{pt})$ (ft)	234.9	234.5	233.9	234.7	232.9	232.5	231.0	225.6	223.2	219.8
$C + \Delta V^2/2g$ (ft)	25.8	25.8	25.8	25.8	25.8	25.8	25.8	25.8	25.8	25.8
H_t (ft)	260.7	260.3	259.7	260.5	258.7	258.3	256.8	251.4	249.0	245.6
$\frac{2.31}{sp\ gr}(P_{pt})$ (ft)	44.9	42.0	38.7	35.4	32.3	31.5	30.7	29.9	29.1	28.3
Bar. (ft)	46.2	46.2	46.2	46.2	46.2	46.2	46.2	46.2	46.2	46.2
H_{ss} (ft abs)	91.1	88.2	84.9	81.6	78.5	77.7	76.9	76.1	75.3	74.5
ΔP_{vc} (psi)	26.4	26.3	26.1	26.2	26.3	26.1	25.7	26.1	25.8	25.4

Run 4C

P_{dc} (psig)	84.5	84.0	83.8	83.4	83.1	83.1	82.9	82.7	82.2	82.0	81.8	81.2	80.1	78.7	77.7	75.6	73.6
P_{pt} (psig)	12.6	12.1	11.7	11.5	11.2	11.0	10.7	10.5	10.2	10.0	9.7	9.5	9.2	9.0	8.7	8.4	8.2
$P_{dc} - P_{pt}$ (psi)	71.9	71.9	72.1	71.9	71.9	72.0	72.2	72.2	72.0	72.0	72.1	71.7	70.9	69.7	69.0	67.2	65.4
$\frac{2.31}{sp\ gr}(P_{dc}-P_{pt})$ (ft)	232.8	232.8	233.5	233.0	232.8	233.2	233.8	234.0	233.1	233.2	233.4	232.2	229.5	226.0	223.5	217.8	211.8
$C + \Delta V^2/2g$ (ft)	25.8	25.8	25.8	25.8	25.8	25.8	25.8	25.8	25.8	25.8	25.8	25.8	25.8	25.8	25.8	25.8	25.8
H_t (ft)	258.6	258.6	259.3	258.8	258.6	259.0	259.6	259.8	258.9	259.0	259.2	258.0	255.3	251.8	249.3	243.6	237.6
$\frac{2.31}{sp\ gr}(P_{pt})$ (ft)	41.0	39.4	38.1	37.2	36.4	35.6	34.8	34.0	33.2	32.4	31.6	30.8	30.0	29.2	28.4	27.2	26.8
Bar. (ft)	46.5	46.5	46.5	46.5	46.5	46.5	46.5	46.5	46.5	46.5	46.5	46.5	46.5	46.5	46.5	46.5	46.5
H_{ss} (ft abs)	87.5	85.9	84.6	83.7	82.9	82.1	81.3	80.5	79.7	78.9	78.1	77.3	76.5	75.7	74.9	73.7	73.3
ΔP_{vc} (psi)	26.3	26.2	26.4	26.4	26.3	26.3	26.4	26.3	26.5	26.2	26.3	26.2	26.0	25.6	25.4	24.9	25.4

Table 5 (continued)

Run 5																	
P_{dc} (psig)	71.6	70.9	70.0	68.3	68.2	67.8	67.4	67.2	66.3	66.1	65.9	65.3	65.0	63.5	62.1	60.8	59.3
P_{pt} (psig)	9.9	9.0	8.0	6.7	6.5	6.2	6.0	5.7	5.2	5.0	4.7	4.2	4.0	3.7	3.5	3.2	3.0
$P_{dc} - P_{pt}$ (psi)	61.7	61.9	62.0	61.6	61.7	61.6	61.4	61.5	61.1	61.1	61.2	61.1	61.0	59.8	58.6	57.6	56.3
$\frac{2.31}{sp\ gr}(P_{dc} - P_{pt})$ (ft)	199.0	199.7	200.0	198.7	199.3	198.7	198.4	198.4	197.6	197.7	197.8	197.6	197.4	193.4	189.5	186.2	182.2
$C + \Delta V^2/2g$ (ft)	12.4	12.4	12.4	12.4	12.4	12.4	12.4	12.4	12.4	12.4	12.4	12.4	12.4	12.4	12.4	12.4	12.4
H_t (ft)	211.4	212.1	212.4	211.1	211.7	211.1	210.8	210.8	210.0	210.1	210.2	210.0	209.8	205.8	201.9	198.6	194.6
$\frac{2.31}{sp\ gr}(P_{pt})$ (ft)	32.1	29.0	25.8	21.8	20.9	20.1	19.3	18.5	16.9	16.1	15.3	13.7	12.9	12.1	11.3	10.5	9.7
Bar. (ft)	46.1	46.1	46.1	46.1	46.1	46.1	46.1	46.1	46.1	46.1	46.1	46.1	46.1	46.1	46.1	46.1	46.1
H_{ss} (ft abs)	78.2	75.1	71.9	67.9	67.0	66.2	65.4	64.6	63.0	62.2	61.4	59.8	59.0	58.2	57.4	56.6	55.8
ΔP_{vc} (psi)	12.5	12.8	12.8	12.6	12.6	12.7	12.7	12.4	12.7	12.7	12.6	12.9	13.1	13.0	12.4	12.2	12.1

Table 6. Venturi Temperature-Multiplier

Temperature, t (°F)	TM	$(TM_t/TM_{1500°F})$	$(TM_t/TM_{1500°F})^2$
140	0.8414	0.832	0.6922
190	0.849	0.8397	0.7051
1500	1.011		

APPENDIX C

VENTURI METER TEMPERATURE-MULTIPLIER

The standard venturi meter flow-rate equation for flow rate at temperature, t, may be written

(1) $$Q_t = k \frac{A_t}{\sqrt{\text{sp gr}_t}} \sqrt{\Delta P_v} \ ,$$

where

$$k = \frac{c}{\sqrt{1-\beta^4}} \sqrt{\frac{2g}{62.37}} \ .$$

Also the flow rate at a base temperature, bt, may be written

(2) $$Q_{bt} = \frac{A_{bt}}{\sqrt{\text{sp gr}_{bt}}} \sqrt{\Delta P_v} \ .$$

Multiplication of equation (1) by unity, which in this case is $\left(\frac{A_{bt}}{A_{bt}}\right) \frac{\sqrt{\text{sp gr}_{bt}}}{\sqrt{\text{sp gr}_{bt}}}$, and regrouping, will give

(3) $$Q_t = \frac{A_t}{A_{bt}} \frac{\sqrt{\text{sp gr}_{bt}}}{\sqrt{\text{sp gr}_t}} \text{k} \frac{A_{bt}}{\sqrt{\text{sp gr}_{bt}}} \sqrt{\Delta P_v} \ ,$$

from which

(4) $$Q_t = K(TM) \sqrt{\Delta P_v} \ ,$$

where

$$K = \frac{kA_{bt}}{\sqrt{\text{sp gr}_{bt}}} \ , \quad \text{and}$$

$$TM = \left(\frac{D_t}{D_{bt}}\right)^2 \frac{\sqrt{\text{sp gr}_{bt}}}{\sqrt{\text{sp gr}_t}} \ .$$

From reference (7), and for a base temperature of 1400°F,

$$K = 84.18 \ , \quad \text{and}$$
$$TM = 1.000 \ .$$

Table 6 presents several temperature multipliers of interest.

The NaK flow rate should equal a previously established water flow rate when

(5) $$(\Delta P_v)_{NaK} = \left(\frac{TM_w}{TM_{NaK}} \right)^2 (\Delta P_v)_w \; ,$$

where subscript w refers to water and subscript NaK refers to the sodium-potassium alloy.

APPENDIX D

PUMP HEAD EQUATIONS

The pump head and the static head at pump suction for water and for NaK were calculated by using the following equations. In the pump head equation for water, the constant 3 represents an elevation correction to the discharge pressure gage. In the pump head equation for the alloy, the symbol C represents a flow-rate-dependent correction to the measured discharge pressure. The locations of the discharge pressure tap for NaK testing and water testing differed, but data were obtained for both taps during water testing.

For water,

$$H_t = \frac{2.31}{\text{sp gr}}(P_{dc} - P_{pt}) - 3 + 1.127(10^{-4})\,Q^2 \quad , \text{ and} \tag{6}$$

$$H_{ss} = \frac{2.31}{\text{sp gr}} P_{pt} + \text{Bar.} \tag{7}$$

For NaK,

$$H_t = \frac{2.31}{\text{sp gr}}(P_{dc} - P_{pt}) + C + 1.127(10^{-4})\,Q^2 \quad , \text{ and} \tag{8}$$

$$H_{ss} = \frac{2.31}{\text{sp gr}} P_{pt} + \text{Bar.} \tag{9}$$

GLOSSARY

N	pump speed, rpm
Q	pump flow, gpm
T	temperature of flowing liquid, °F
P_d	pump discharge pressure, psig
P_{dc}	corrected pump discharge pressure, psig
P_{pt}	pump suction static pressure, psig
P_p	venturi upstream pressure, psig
P_t	venturi throat pressure, psig
ΔP_v	venturi differential pressure, psi
ΔP_{vc}	corrected venturi differential pressure, psi
H_t	pump total head, ft
H_{ss}	static head at pump suction, ft abs
H_{vp}	vapor pressure of liquid, ft
H_{ci}	static head at pump suction at cavitation inception, ft abs
C	pump discharge pressure gage correction, ft
Bar.	barometric pressure, ft
sp gr	specific gravity of flowing liquid
TM	venturi temperature multiplier
c	venturi coefficient-of-discharge
g	acceleration of gravity, 32.2 ft/sec^2
A	venturi throat area, ft^2
D	venturi throat dia, ft
β	ratio of venturi throat to pipe diameters
V	velocity in the suction pipe

ACKNOWLEDGMENTS

The author wishes to express his appreciation to Dr. George F. Wislicenus, Pennsylvania State University, for suggesting the problem and its possible value.

Special acknowledgment is due H. W. Savage, Reactor Projects Division, ORNL, and to E. R. Dytko.

The author is indebted to Professor W. K. Stair, Mechanical Engineering Department, University of Tennessee, for his counsel and guidance during the course of the problem.

The continuing support and the constructive criticism of L. V. Wilson, Design Department, Reactor Projects Division of Oak Ridge National Laboratory, are gratefully recognized.

Special recognition is extended to H. C. Young and J. N. Simpson, and to D. L. Gray, Experimental Engineering Department, Reactor Projects Division, for their assistance and cooperation in obtaining water test and elevated temperature test data.